Journal of Alloys and Compounds 513 (2012) 213–219

Contents lists available at SciVerse ScienceDirect

Journal of Alloys and Compounds

journal homepage: www.elsevier.com/locate/jallcom

MOX (M = Zn, Co, Fe)/AP shell–core nanocomposites for self-catalytical decomposition of ammonium perchlorate

Zhaoxia Zhou[a], Shouqin Tian[b], Dawen Zeng[a,b,*], Gen Tang[b], Changsheng Xie[b]

[a] State Key Laboratory of Material Processing and Die & Mould Technology, Huazhong University of Science and Technology, Wuhan 430074, PR China
[b] Nanomaterials and Smart Sensor Research Laboratory, Department of Materials Science and Engineering, Huazhong University of Science and Technology, Wuhan 430074, PR China

ARTICLE INFO

Article history:
Received 6 August 2011
Accepted 7 October 2011
Available online 17 October 2011

Keywords:
MOX/AP
Shell–core nanocomposites
Self-catalytical decomposition
Nanocatalysts

ABSTRACT

To overcome the agglomeration of metal oxide (MOX) nanocatalysts mechanically mixed with ammonium perchlorate (AP) and other additives of rocket propellant, the shell–core nanocomposites of MOX/AP have been synthesized successfully by a facile liquid deposition method at room temperature. SEM analysis revealed that MOX (M = Zn, Co, Fe) nanoparticles were deposited on the surface of AP particles as either a continuous thin layer or small clusters. Owing to the existence of the shell of MOX nanocatalysts, ZnO/AP, Co_3O_4/AP and Fe_2O_3/AP nanocomposites showed excellent self-catalytic performances for AP thermal decomposition: lowering the decomposition temperature from 398 °C to 272 °C, 285 °C, 337 °C, and increasing the heat release from 584 J g^{-1} to 1137 J g^{-1}, 1237 J g^{-1}, 1010 J g^{-1}, respectively. Moreover, their self-catalytic performances mainly relied on the content of MOX nanocatalysts, which was controlled by the concentration of metal salts in the precursor solution. In particular, ZnO/AP nanocomposites with the mass ratio of ZnO:AP = 4:100 exhibited the best self-catalytic performance in decreasing the activation energy from 154.0 kJ/mol to 96.5 kJ/mol. The MOX/AP (M = Zn, Co, Fe) shell–core nanocomposites could have a promising application in the rocket propellant for improving the thermal-catalytic decomposition performance of AP.

1. Introduction

As a key energetic material and main oxidizing agent for rocket technologies, ammonium perchlorate (AP) continues to inspire new research efforts to investigate its thermal decomposition process, which is remarkably sensitive to the additives [1,2]. Many scholars have studied a variety of the additives to enhance their catalytic properties for AP decomposition. Among these additives, metal oxides (MOXs) are used widely as a kind of efficient catalysts accelerating the thermal decomposition of AP [3–9].

Due to much higher catalysis efficiency of nanoparticles, many researchers have turned their attention to MOX nanocatalysts rather than MOX microcatalysts to catalyze AP thermal decomposition [10–12]. However, owing to their high surface activity, MOX nanocatalysts are apt to agglomerate so that they are difficult to mix uniformly with AP and other rocket fuel additives by conventional mechanical mixing technology, resulting in a decrease of their catalytic activity [13,14]. To improve the dispersion of nanocatalysts in the mixture, ferrocene and its derivatives have also been studied as catalysts due to their low melting points. They would be melted into liquid and then evenly coated on the AP surface to form shell–core structure at the elevated temperatures, effectively promoting the thermal decomposition of AP. Unfortunately, the use of ferrocene and its derivatives as the high-burning-rate catalysts results in some setbacks such as their tendency towards migration in the bulk of the material, their sensitivity towards oxidation by air and their evaporation loss during processing [15–17]. To overcome the setbacks, MOX nanoparticles are expected to form the external shell instead of ferrocene and its derivatives so that the shell–core nanocomposites of MOX/AP are produced and may also avoid the agglomeration of MOX nanocatalysts and further improve their catalytic efficiency for the thermal decomposition of AP.

As we know, the shell–core nanocomposites fabricated by templating the organic or inorganic cores exhibit very fine dispersion and stability, strong interactions at the interface, which are very beneficial for the properties of the composites [18–22]. For example, to overcome the agglomeration of the carbon nanotubes (CNTs) in Al matrix by traditional mechanical mixing technology, He et al. have synthesized a novel CNT(Ni)–Al composite, in which the in situ synthesized CNTs were very homogeneously dispersed in the Al powders with strong interactions at the interface [23]. In addition, polystyrene–ZnO composite particles with core–shell or raspberry-like morphology have been prepared by Agrawal et al.,

* Corresponding author at: Nanomaterials and Smart Sensor Research Laboratory, Department of Materials Science and Engineering, Huazhong University of Science and Technology, Wuhan 430074, PR China. Tel.: +86 027 87556544; fax: +86 027 87543778.
E-mail address: dwzeng@mail.hust.edu.cn (D. Zeng).

0925-8388/$ – see front matter.
doi:10.1016/j.jallcom.2011.10.021

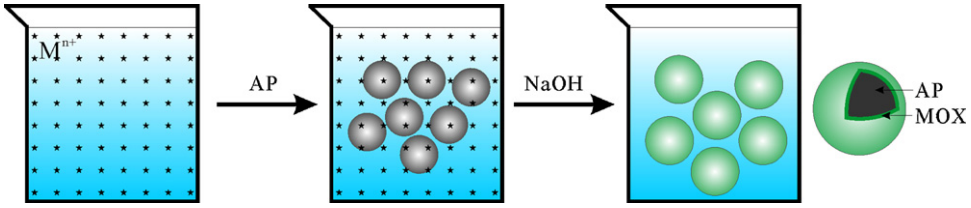

Scheme 1. Schematic presentation of in situ synthesis of MOX/AP nanocomposites with shell–core structure.

which showed a finer dispersion and stabilization and provided a larger number of active sites than the corresponding bulk components [24]. However, there have been no reports of the shell–core nanocomposites of MOX/AP because AP is highly soluble in many solvents and shows poor thermal stability above 150 °C. Therefore, it is still a great challenge to develop a facile method for preparing MOX/AP shell–core nanocomposites.

In this study, AP powders were successfully covered by MOX nanoparticles to form the shell–core structure by a facile liquid deposition method at room temperature. One of the most important characteristics of the preparation is that the MOX nanoparticles in situ grew and coated homogeneously on the surface of the AP powders. The obtained ZnO/AP, Co_3O_4/AP, Fe_2O_3/AP nanocomposites all showed excellent self-catalytic effects for the thermal decomposition of AP in lowering the decomposition temperature and increasing the heat release. Moreover, by adjusting the concentration of metal salts in the precursor solution, the thickness of the shell formed by MOX nanocatalysts in MOX/AP nanocomposites could be changed, accompanied with the variance in their self-catalytic performance for the thermal decomposition of AP.

2. Experimental procedure

2.1. Sample preparation

Zinc chloride ($ZnCl_2$) (98.0%), cobalt nitrate hexahydrate ($Co(NO_3)_2{\cdot}6H_2O$) (99.0%), ferric chloride anhydrous ($FeCl_3$) (97%), ethyl acetate ($CH_3COOC_2H_5$) (99.5%), AP (AR, d_{50}: 140 μm) and sodium hydroxide (NaOH) (96%), were all purchased from Sinopharm Chemical Reagent Co. Ltd. (China) and used as received without further purification.

Our approach to a novel fabrication process for MOX/AP shell–core nanocomposites principally consists of in situ synthesis of MOX nanoparticles by templating the AP cores. The selection of solvent is critical in our experiments. In the selected solvent, AP must be insoluble, but the metal salt can be dissolved. Ethyl acetate meets the mentioned conditions and is selected as a solvent. A typical preparation procedure mainly includes three steps as shown by Scheme 1, and the synthesis conditions of different samples are listed in Table 1. In the first step, a certain amount of $FeCl_3$, $Co(NO_3)_2{\cdot}6H_2O$, $ZnCl_2$ salt was dissolved in 60 mL $CH_3COOC_2H_5$ respectively to produce the corresponding solution with given concentration. Secondly, 2 g AP powders were added into the solution as a template, followed by vigorous stirring to make AP powders distribute in the solution homogeneously. Subsequently, a desired volume of 0.5 M NaOH solution was added into the above mixture drop by drop to make sure the metal ions in the solution could react with NaOH completely to produce precipitation. According to the principle of heterogeneous nucleation, the MOX nanocrystals would preferentially be nucleated and then grow up on the surface of AP, constituting the composites with shell–core structure. Then the products were filtered to obtain the nanocomposites and then dried at 80 °C in an electric oven. The color of S1(ZnO/AP), S2(Co_3O_4/AP) and S3(Fe_2O_3/AP) nanocomposites was white, cyan and tan, respectively. This deposition–precipitation is suggested as a preparation method for getting highly dispersed catalysts with strong interactions at the interface between surface catalysts and the support, which is very beneficial for the catalytic properties of the subsequent composites [25]. In addition, the content of MOX nanoparticles or shell thickness is dependent on the mass ratio of MOX nanoparticles to AP powders, which can be adjusted by the concentration of the metal ions in the precursor solution. The ZnO/AP shell–core samples (S4, S5) with different mass ratios (or shell thickness) were prepared according to the synthesis conditions given in Table 1.

2.2. Characterization

The morphologies of the MOX/AP shell–core nanocomposites were observed by field-emission scanning electron microscopy (FESEM FEI Sirion 200) equipped with an energy dispersion X-ray spectrometer (EDS), operated at an acceleration voltage of 20.0 kV, and their chemical compositions were determined by EDS. The crystal phase structures of the products were analyzed by PANalytical X'Pert PRO diffractometer (XRD) using Cu Kα1 radiation (λ = 1.5406 Å) in the 2θ range from 20° to 70°. There are no signals of other matter except AP in the XRD patterns of the products because the content of MOX nanoparticles in the nanocomposites is lower than the detectable limit of XRD (5 wt%). To study the phase structure of MOX nanoparticles by XRD, the nanocomposites were washed with distilled water for several times to dissolve AP completely and then the remains were MOX nanoparticles.

2.3. Activity

All as-prepared nanocomposites were characterized by TG–DTA test using Diamond TG/DTA in N_2 atmosphere over the temperature range of 30–500 °C without lids to investigate their self-catalytic performance in the thermal decomposition of AP. A total sample mass of 3.0 mg was used for all runs. To investigate the catalytic effect of MOX nanoparticles on AP decomposition, S1 (ZnO/AP), S2 (Co_3O_4/AP) and S3 (Fe_2O_3/AP) nanocomposites were studied by TG–DTA at a constant heating rate of 10 K/min to compare their decomposition temperature and heat release. In addition, to study the influence of the content of MOX nanoparticles or the shell thickness on the performance of self-catalytic decomposition, S1 (ZnO:AP = 4:100), S4 (ZnO:AP = 2:100) and S5 (ZnO:AP = 6:100) were also tested by TG–DTA at a heating rate of 10 K/min. Furthermore, the activation energies of AP decomposition with ZnO/AP shell–core nanocomposites (S1, S4, S5) were measured by varying the heating rates from 2 to 20 K/min.

3. Results and discussion

3.1. Morphology and structure of MOX/AP shell–core nanocomposites

Fig. 1 shows FESEM images of the uncoated AP and S1 (ZnO/AP), S2 (Co_3O_4/AP), S3 (Fe_2O_3/AP) nanocomposites. The pure AP particles are uniform with the average diameter of about 140 μm (Fig. 1a), and the surface of the uncoated AP is very smooth and clean in the enlarged image (Fig. 1b). Compared with the pure AP, the surface of all the nanocomposites is rough, indicating that MOX

Table 1
The synthesis conditions and self-catalytic properties of MOX/AP samples.

Sample	Type of salt	Mass ratio MOX:AP[a]	Concentration of salt (mol/L)	Volume of 0.05 M NaOH (mL)	Decomposition temperature (°C)	Heat release (J/mol)	E_a (kJ/mol)	ln$A$
AP	–	–	–	–	397	584	154.0 ± 13.9	26.8
S1	$ZnCl_2$	4:100	0.016	4	272	1137	96.5 ± 15.0	20.0
S2	$Co(NO_3)_2{\cdot}6H_2O$	4:100	0.016	4	285	1237	–	–
S3	$FeCl_3$	4:100	0.016	6	337	1010	–	–
S4	$ZnCl_2$	2:100	0.008	2	276	1131	93.7 ± 22.4	18.4
S5	$ZnCl_2$	6:100	0.024	6	293	986	142.1 ± 21.0	29.4

[a] The mass ratio MOX:AP is based on two assumptions: (1) all the M^{n+} ions in the solution were converted into the MOX nanocatalysts; (2) all the MOX nanoparticles were coated on the AP surface.

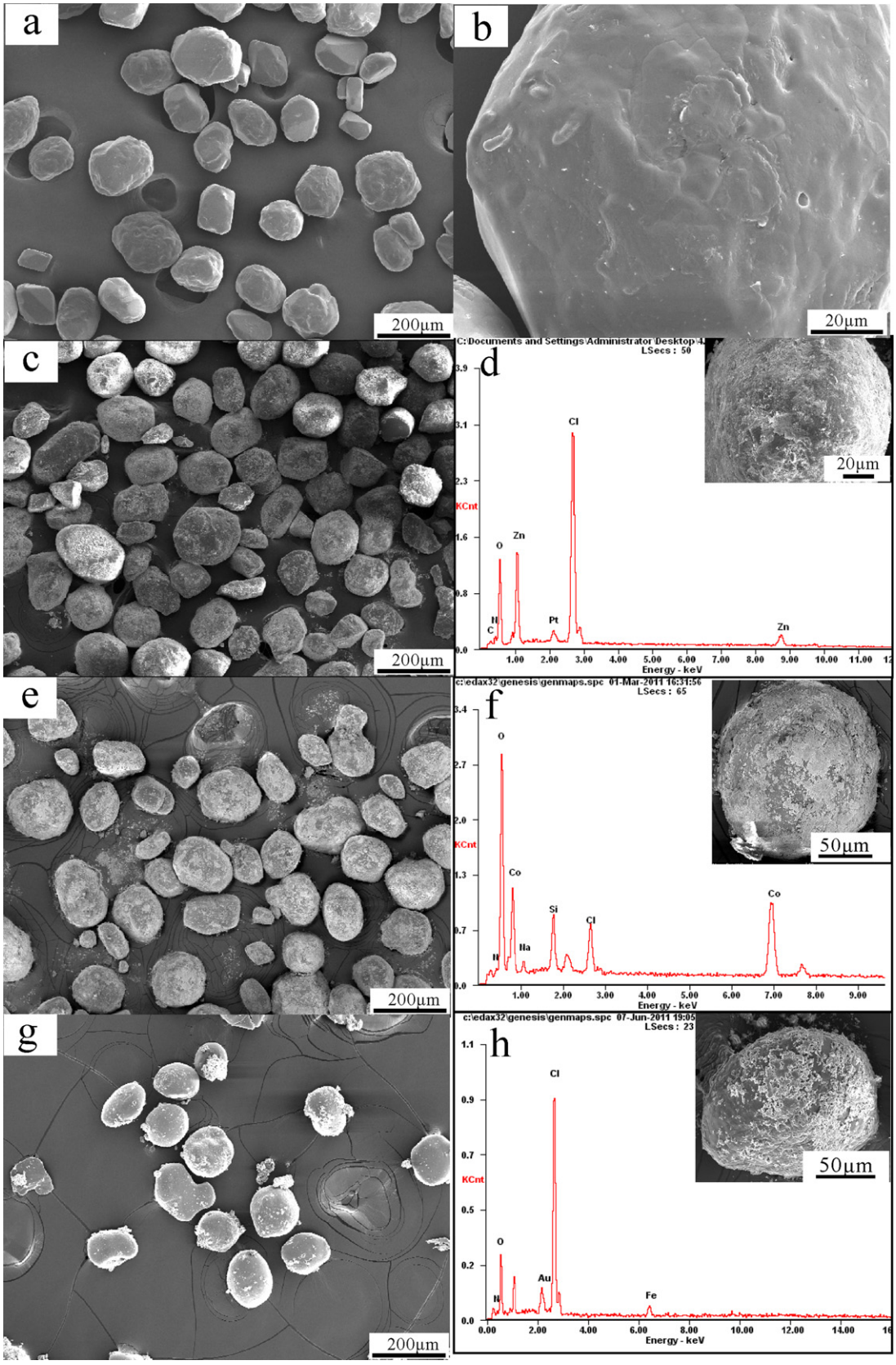

Fig. 1. SEM and EDX images of pure AP (a and b) and the as-prepared MOX (M = Zn, Co, Fe)/AP shell–core nanocomposites: (c and d) S1 (ZnO/AP); (e and f) S2 (Co_3O_4/AP); (g and h) S3 (Fe_2O_3/AP).

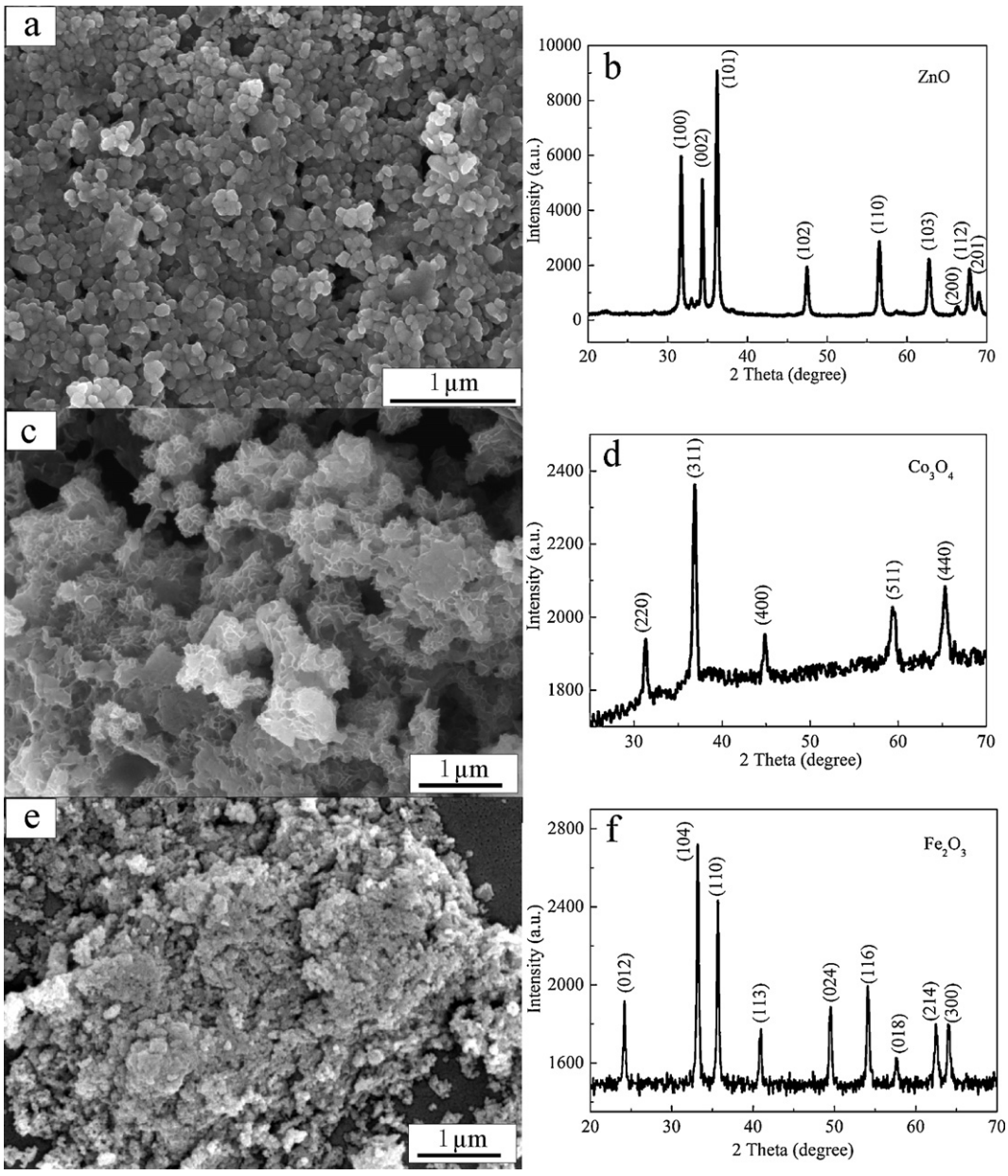

Fig. 2. XRD patterns and SEM images of the as-prepared shells of (a and b) S1 (ZnO/AP), (c and d) S2 (Co_3O_4/AP) and (e and f) S3 (Fe_2O_3/AP).

nanoparticles homogeneously grew and coated on the surface of AP to produce shell–core structure as shown in Fig. 1c, e and g. To obtain the elemental composition of the MOX/AP shell–core nanocomposites, EDS has also been carried out. The results in Fig. 1d, f and h demonstrate that shell–core MOX/AP contains the elements of N, O, Cl and Zn/Co/Fe, indicating that the shell on the AP surface may be MOX nanoparticles, which can catalyze the thermal decomposition of AP.

To further investigate the microstructure of MOX nanoparticles on the AP surface, the MOX/AP nanocomposites were washed by distilled water for removing AP. Fig. 2 shows SEM and XRD patterns of the MOX (M = Zn, Co, Fe) nanoparticles. XRD patterns show that the phase of the shell in S1, S2 and S3 samples is ZnO, Co_3O_4 and Fe_2O_3 respectively, and all diffraction peaks are in good agreement with the standard diffraction data for the ZnO (JCPDS 36-1451), Co_3O_4 (JCPDS 09-0418) and Fe_2O_3 (JCPDS 33-0664), respectively. Also, it is observed that the ZnO nanoparticles display a good crystallinity while the other two do not. SEM analysis revealed that the size of MOX (ZnO, Co_3O_4, and Fe_2O_3) particles is about approximately 100 nm. Both the ZnO and Fe_2O_3 nanoparticles are uniformly granular, and Co_3O_4 nanoparticles are flower-like.

In addition, the content of MOX nanoparticles or thickness of the coating shell can be tuned by the concentration of the metal ions in the precursor solution. As shown in Fig. 3, with a lower Zn^{2+} concentration, sparser ZnO nanocrystals (S4) can be obtained on the surface of AP; with a higher Zn^{2+} concentration, the AP particles were completely covered with the denser ZnO nanocrystals (S5) to produce the shell–core structure. The results suggest that the shell thickness or the content of ZnO nanoparticles is increased with an increase of Zn^{2+} concentration, which may have an important influence on the self-catalytic properties of the nanocomposites.

3.2. The self-catalytic activity of MOX/AP composites for thermal decomposition of AP

The self-catalytic properties of MOX/AP (M = Zn, Co, Fe) nanocomposites in the thermal decomposition of AP were

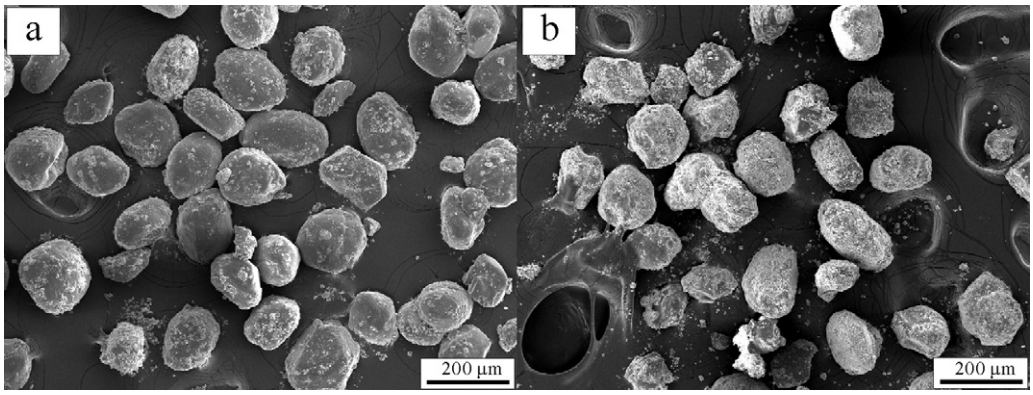

Fig. 3. FESEM images of (a) S4 (ZnO:AP = 2:100) and (b) S5 (ZnO:AP = 6:100).

investigated by TG–DTA measurements at a heating rate of 10 K/min. Fig. 4 shows the DTA and TG curves of pure AP and the as-prepared nanocomposites. All DTA curves show an endothermic peak at about 245 °C, which is attributed to the crystal transformation of AP from orthorhombic to cubic phase. For the uncoated AP, there are two obvious exothermic peaks centered at about 298 °C and 397 °C, which correspond to the low-temperature decomposition (LTD) and high-temperature decomposition (HTD), respectively. As shown in the TG curve, 30% weight loss at LTD indicates the partial decomposition of AP and 70% weight loss at HTD means the complete decomposition of AP. It is well established that LTD involves a heterogeneous process which includes proton transfer in the AP subsurface to yield NH_3 and $HClO_4$ [1,2,26], the capture of $HClO_4$ by proton trap ClO_3 in the defect-bearing site of the lattice, and finally the decomposition of $HClO_4$ and reaction with NH_3. Alternatively, HTD is associated with the simultaneous dissociation and sublimation of AP to $HClO_{4(g)}$ and $NH_{4(g)}$. The total process can be expressed as follows:

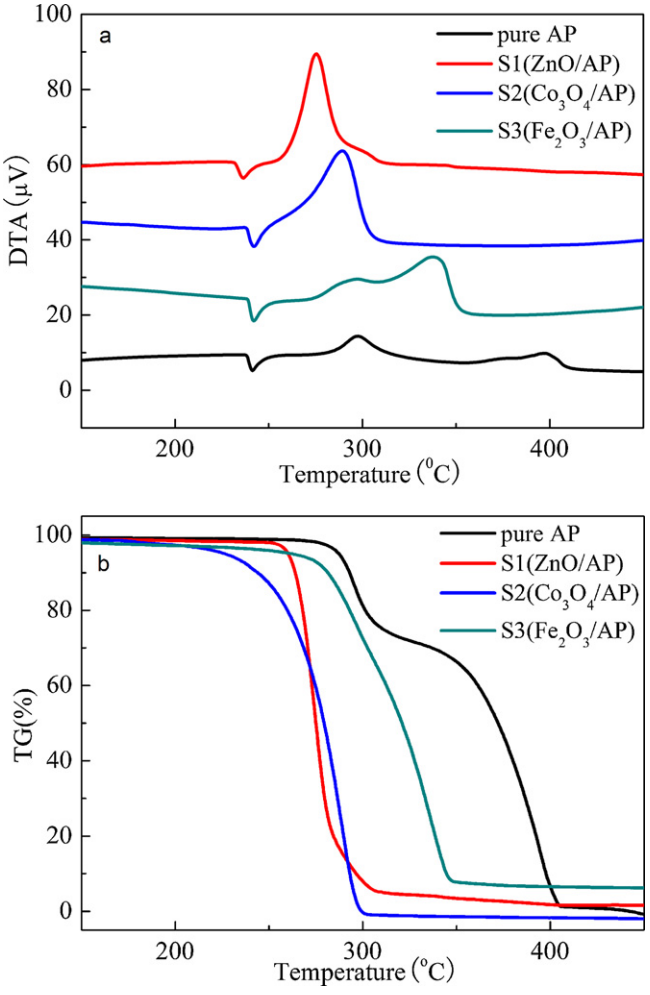

Fig. 4. (a) TG and (b) DTA curves of pure AP, S1 (ZnO/AP), S2 (Co_3O_4/AP) and S3 (Fe_2O_3/AP).

$$NH_4ClO_4 \leftrightarrow NH_3\text{-}H\text{-}ClO_4 \leftrightarrow NH_3\text{-}HClO_4 \leftrightarrow NH_{3(a)} + HClO_{4(a)} \quad (LTD) \tag{1}$$

$$NH_{3(a)} + HClO_{4(a)} \leftrightarrow NH_{3(g)} + HClO_{4(g)} \quad (HTD) \tag{2}$$

For ZnO/AP and Co_3O_4/AP nanocomposites, a significant difference for AP decomposition with and without catalysts was the disappearance of HTD, which should be associated with the reduction in the concentration of $NH_{3(a)}$ and $HClO_{4(a)}$ [4], and there was only one exothermic peak which was significantly reduced. However, it was found that Fe_2O_3/AP nanocomposites did not shift the LTD exothermic peak and showed a weak endothermic peak much closer to the LTD peak that was observed for pure AP, which was consistent with the previous report [3]. Furthermore, all kinds of MOX/AP nanocomposites could dramatically decrease the decomposition temperature of AP and increase the heat release. As shown in Table 1, the shell–core nanocomposites of ZnO/AP, Co_3O_4/AP, Fe_2O_3/AP led to a significant reduction of decomposition temperature from 398 °C to 272 °C, 285 °C, 337 °C, and an increase of heat release from 584 J g^{-1} to 1109 J g^{-1}, 1237 J g^{-1}, 1010 J g^{-1}, correspondingly. The result clearly indicates that these MOX/AP nanocomposites have a good self-catalytic performance for the thermal decomposition of AP, and the order of self-catalytic activity observed during thermal ignition is shown as follows: ZnO/AP > Co_3O_4/AP > Fe_2O_3/AP. Intrinsically, the thermal decomposition of AP is closely associated with the chemical nature of the nanocrystal additives [27], although there still remain some unsolved issues. The different influences of MOX/AP nanocomposites in self-catalytic reactions involving charge transfer may be connected with the different electrical properties of the additives [28,6].

In particular, for the ZnO/AP nanocomposites, AP could be decomposed at a temperature as low as 272 °C, which is much lower than those catalyzed by ZnO twin-cones, single-cage ZnO nanorod-assembled superstructure, and other additive such as Fe_2O_3, Co_3O_4, and metal Ni recently reported in the literature [3–5,29,30]. In fact, the in situ synthesized MOX nanocatalysts are homogeneously distributed on the surface of AP to overcome the MOX agglomeration for the conventionally mechanical mixture. On the other hand, the

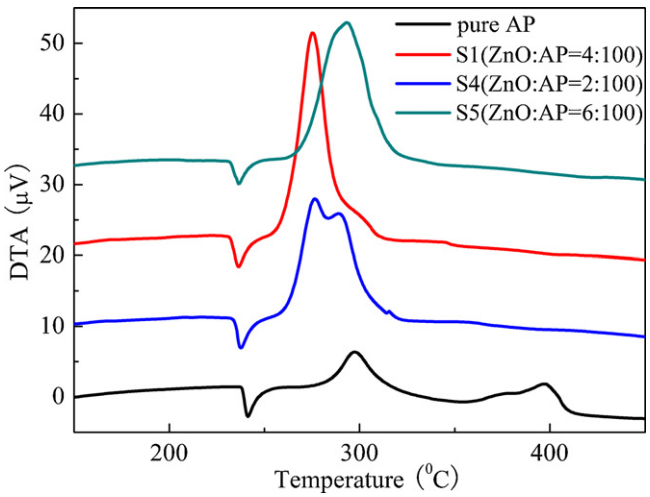

Fig. 5. DTA curves of pure AP, S1 (ZnO:AP = 4:100), S4 (ZnO:AP = 2:100) and S5 (ZnO:AP = 6:100).

gas reactant molecules produced by the decomposition of AP can directly contact with active site of the catalysts to cause adsorption reaction i.e. the catalytic active center can take part in the reaction, thus markedly enhancing the self-catalytic activity of ZnO/AP nanocomposites in the thermal decomposition of AP [31].

As reported previously [5,32], thermally catalytic decomposition of AP is also highly dependent on the amounts of catalyst loaded. The self-catalytic activities of ZnO/AP nanocomposites with different mass ratios of ZnO nanocatalysts to AP powders from 2:100 (S4) to 6:100 (S5) were investigated by DTA measurements. The DTA curves (Fig. 5) show that only one obvious exothermic peak was observed for S1 (ZnO:AP = 4:100) and S5, comparing with two exothermic peaks for pure AP and S4. According to data in Table 1, increasing or decreasing the content of ZnO nanocatalyst in the composites will both lead to an increase of decomposition temperature and a decrease of heat release, thus reducing the self-catalytic activity [32]. Specifically, S1 exhibits the best self-catalytic performance in decreasing the maximum AP decomposition temperature to 272 °C and increasing the decomposition heat to 1137 J g^{-1} without lids.

To further study the influence of the mass ratio of MOX nanocatalysts to AP powders on the self-catalytic properties for the thermal decomposition of AP, pure AP, S1, S4 and S5 were investigated by DTA test at different heating rates from 2 to 20 K/min, respectively. As shown in Fig. 6, the decomposition temperature of AP with or without ZnO catalysts is dependent on the heating rate and a slight increase in the temperature of both LTD and HTD process was accompanied with the increase of heating rate. The kinetic parameters for AP decomposition with ZnO/AP nanocomposites could be calculated from the exothermic peak temperature dependence as a function of heating rate. The relationship between decomposition temperature and heating rate can be described by Kissinger correlation:

$$\ln\left(\frac{\beta}{T_p^2}\right) = \ln\left(\frac{AR}{E_a}\right) - \frac{E_a}{RT_p} \quad (3)$$

In this correlation, β is the heating rate in degree Celsius per minute, T_p is the peak temperature, R is the ideal gas constant, E_a is the activation energy, and A is the pre-exponential factor. According to Eq. (3), the term $\ln \beta/T_p^2$ varies linearly with $1/T_p$, yielding the kinetic parameters of activation energy from the slope of the straight line and of pre-exponential factor from the intercept [4]. Fig. 7 shows the experimentally measured $\ln \beta/T_p^2$ versus $1/T_p$ with

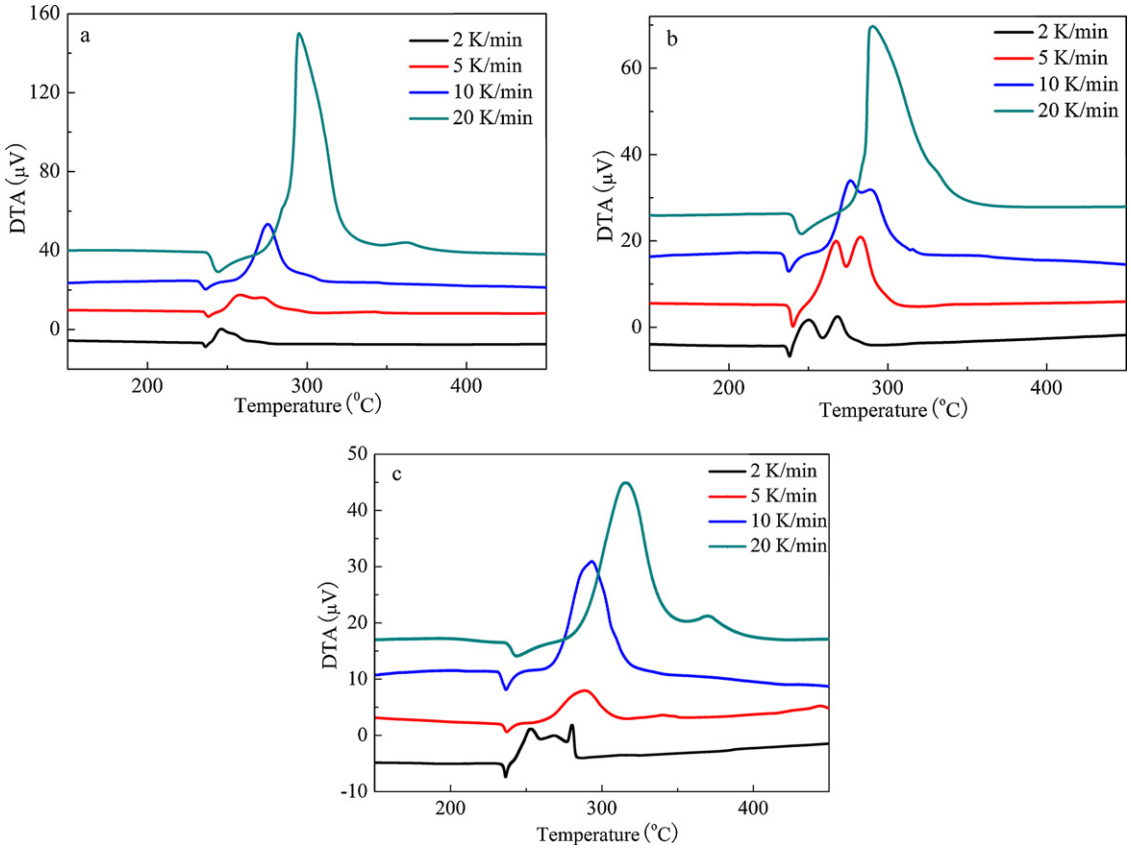

Fig. 6. DTA curves of (a) S1 (ZnO:AP = 4:100), (b) S4 (ZnO:AP = 2:100) and (c) S5 (ZnO:AP = 6:100) at different heating rates.

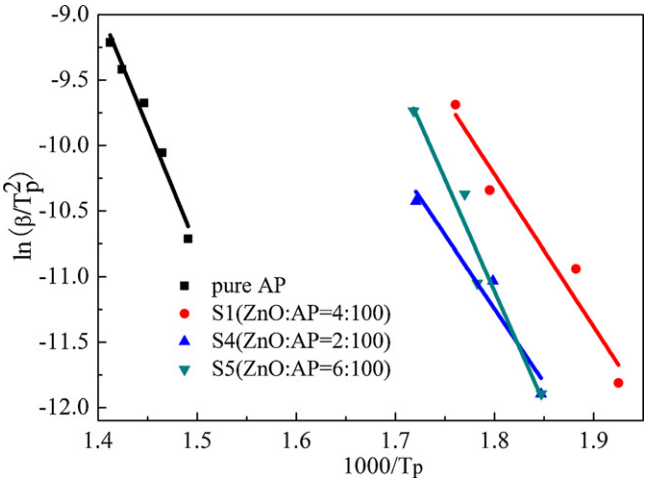

Fig. 7. Dependence of $\ln(\beta/T_p)$ on $1/T_p$ for AP, S1 (ZnO:AP = 4:100), S4 (ZnO:AP = 2:100) and S5 (ZnO:AP = 6:100). Scatter points are experimental data and lines denote the liner fitting results.

and without ZnO additives. As shown in Table 1, for pure AP, the activation energy of HTD was calculated to be 154.0 ± 13.9 kJ/mol, which is close to the value previously reported in literature [5]. In the presence of ZnO/AP nanocomposites, the activation energy of AP decomposition became as small as E_a = 93.7 ± 22.4 kJ/mol with S4 (ZnO:AP = 2:100), 96.5 ± 15.0 kJ/mol with S1 (ZnO:AP = 4:100) or 142.1 ± 21.0 kJ/mol with S5 (ZnO:AP = 6:100). It is seen that the activation energy is increased with an increase of the content of ZnO nanocatalysts in the nanocomposites. The increased activation energy for AP decomposition is caused by the kinetic compensation effect [33]. However, the activation energy of AP decomposition is not the only parameter that describes the decomposition process, the value of pre-exponential factor should also be considered. For the reaction system in which compensation effect affects the decomposition behavior significantly, the value of ln$A$ is 26.8, 18.4, 20.0, 29.4 for pure AP, S4, S1 and S5, respectively. Usually, a smaller value of ln$A$ means better catalytic activity of the catalysts. Obviously, S4 and S1 show better catalytic activities towards AP decomposition than S5. It can be concluded that increasing the proportion of the MOX nanocatalyst in the nanocomposites will affect its catalytic effect. In addition, both the activation energy and pre-exponential factor of S4 and S1 are basically the same, but there are two exothermic peaks for S4 while only one exothermic peak is observed for S1 in the DTA curves as shown in Fig. 5 so that S1 can show more concentrated heat release than S4. Therefore, ZnO/AP nanocomposites with the mass ratio of ZnO:AP = 4:100 (S1) exhibited the best self-catalytic performance in the thermal decomposition of AP.

4. Conclusion

The shell–core nanocomposites of MOX/AP (M = Zn, Fe, Co) were successfully synthesized by a facile liquid deposition method at room temperature for enhancing their self-catalytic properties in the thermal decomposition of AP. The in situ synthesized MOX nanoparticles were coated on the surface of AP homogeneously to form shell–core structure for avoiding the agglomeration of MOX nanocatalysts during the mechanical mixing process. It was found that all the ZnO/AP, Co_3O_4/AP, Fe_2O_3/AP nanocomposites showed significant self-catalytic effects in lowering the decomposition temperature and increasing the heat release. Moreover, the content of MOX nanoparticles or the shell thickness could be adjusted by changing the concentration of metal salts in the precursor solution, accompanied by the variation of the self-catalytic properties of the MOX/AP nanocomposites. Also, the TG/DTA results of ZnO/AP nanocomposites with different mass ratios indicated that ZnO/AP nanocomposites with the mass ratio of 4:100 exhibited the best self-catalytic performance in the thermal decomposition of AP. This work could provide an effective method for preparing MOX/AP shell–core nanocomposites to improve the dispersion of the MOX nanocatalysts in the mixture, and then enhance the performance of rocket propellants.

Acknowledgments

The authors gratefully acknowledge the financial support by the National Basic Research Program of China (Grant Nos. 2009CB939705 and 2009CB939702), the Natural Science Foundation (NSF) of China (Nos. 50772040 and 50927201), and the Opening Research Foundation of State Key Laboratory of Advanced Technology for Materials Synthesis and Processing (Wuhan University of Technology). Also, we thank the technology support by the Analytic Testing Center of HUST for carrying out XRD, FESEM and TG–DTA.

References

[1] V.V. Boldyrev, Thermochim. Acta 443 (2006) 1–36.
[2] S. Vyazovkin, C.A. Wight, Chem. Mater. 11 (1999) 3386–3393.
[3] H. Xu, X.B. Wang, L.Z. Zhang, Powder Technol. 185 (2008) 176–180.
[4] X.F. Sun, X.Q. Qiu, L.P. Li, G.S. Li, Inorg. Chem. 47 (2008) 4146–4152.
[5] L.P. Li, X.F. Sun, X.Q. Qiu, J.X. Xu, G.S. Li, Inorg. Chem. 47 (2008) 8839–8846.
[6] K. Muraleedharan, M.P. Kannan, T. Gangadevi, J. Therm. Anal. Calorim. 100 (2010) 177–181.
[7] L.J. Chen, L.P. Li, G.S. Li, J. Alloys Compd. 464 (2008) 532–536.
[8] G.R. Duan, X.J. Yang, J. Chen, G.H. Huang, L.D. Lu, X. Wang, Powder Technol. 172 (2007) 27–29.
[9] D.L. Reid, A.E. Russo, R.V. Carro, M.A. Stephens, A.R. LePage, T.C. Spalding, E.L. Petersen, S. Seal, Nano Lett. 7 (2007) 2157–2161.
[10] I.P.S. Kapoor, P. Srivastava, G. Singh, Propell. Explos. Pyrotech. 34 (2009) 351–356.
[11] Y.P. Wang, J.W. Zhu, X.J. Yang, L.D. Lu, X. Wang, Thermochim. Acta 437 (2005) 106–109.
[12] N.B. Singh, A.K. Ojha, Thermochim. Acta 390 (2002) 67–72.
[13] Y. Yang, X.J. Yu, J. Wang, Y.X. Wang, J. Nanomater. 2011 (2010) 1–5.
[14] Z.Y. Ma, Propell. Explos. Pyrotech. 31 (2006) 447–451.
[15] Y. Gao, H.D. Li, C.F. Ke, L.L. Xie, B. Wei, Y.F. Yuan, Appl. Organomet. Chem. 25 (2011) 407–411.
[16] D. Saravanakumar, N. Sengottuvelan, V. Narayanan, M. Kandaswamy, T.L. Varghese, J. Appl. Polym. Sci. 119 (2011) 2517–2524.
[17] F.J. Xiao, M.M. Shi, L. Peng, Y.J. Luo, J.C. Zhao, J. Inorg. Organomet. Polym. 21 (2011) 175–181.
[18] N. Zhang, S.Q. Liu, X.Z. Fu, Y.J. Xu, J. Phys. Chem. C 115 (2011) 9136–9145.
[19] C.W. Chen, T. Serizawa, M. Akashi, Chem. Mater. 11 (1999) 1381–1389.
[20] O. Siiman, A. Burshteyn, J. Phys. Chem. B 104 (2000) 9795–9810.
[21] Y.F. Zhang, X.H. Liu, J.R. Nie, L. Yu, Y.L. Zhong, C. Huang, J. Solid State Chem. 184 (2011) 387–390.
[22] C. Li, Z.Y. Ma, L.X. Zhang, R.Y. Qian, Chin. J. Chem. 27 (2009) 1863–1867.
[23] C.N. He, N.Q. Zhao, C.S. Shi, X.W. Du, J.J. Li, H.P. Li, Q.R. Cui, Adv. Mater. 19 (2007) 1128–1132.
[24] M. Agrawal, A. Pich, N.E. Zafeiropoulos, S. Gupta, J. Pionteck, F. Simon, M. Stamm, Chem. Mater. 19 (2007) 1845–1852.
[25] W.J. Shen, Y. Matsumura, J. Mol. Catal. A: Chem. 153 (2000) 165–168.
[26] L. Rosso, M.E. Tuckerman, Solid State Ionics 161 (2003) 219–229.
[27] D.V. Survase, M. Gupta, S.N. Asthana, Prog. Cryst. Growth Charact. 45 (2002) 161–165.
[28] A.A. Said, J. Therm. Anal. 37 (1991) 959–967.
[29] J.Z. Yin, Q.Y. Lu, Z.N. Yu, J.J. Wang, H. Pang, F. Gao, Cryst. Growth Des. 10 (2010) 40–43.
[30] H.Z. Duan, X.Y. Lin, G.P. Liu, L. Xu, F.S. Li, J. Mater. Process. Technol. 208 (2008) 494–498.
[31] M. Zheng, Z.S. Wang, J.Q. Wu, Q. Wang, J. Nanopart. Res. 12 (2010) 2211–2219.
[32] L.L. Liu, F.S. Li, L.H. Tan, L. Ming, Y. Yi, Propell. Explos. Pyrotech. 29 (2004) 34–38.
[33] P.R. Patil, V.N. Krishnamurthy, S.S. Joshi, Propell. Explos. Pyrotech. 31 (2006) 442–446.